Available online at www.sciencedirect.com

SciVerse ScienceDirect

Ceramics International 38 (2012) 5707–5712

CERAMICS INTERNATIONAL

www.elsevier.com/locate/ceramint

Characterization of blue $CoAl_2O_4$ nano-pigment synthesized by ultrasonic hydrothermal method

Jin-Ho Kim [a,*], Bo-Ram Son [a,b], Dae-Ho Yoon [b], Kwang-Taek Hwang [a], Hyung-Goo Noh [c], Woo-Seok Cho [a], Ung-Soo Kim [a]

[a] *Icheon Branch, Korea Institute of Ceramic Engineering & Technology (KICET), Icheon-si, Gyeonggi-do, Republic of Korea*
[b] *School of Advanced Materials Science and Engineering, Sungkyunkwan University, Republic of Korea*
[c] *Department of Design and Craft, Hongik University, Republic of Korea*

Received 1 February 2012; received in revised form 2 April 2012; accepted 3 April 2012
Available online 14 April 2012

Abstract

Nano-sized $CoAl_2O_4$ pigments, which have received significant attention as a coloring agent in glaze and bulk tile compositions, were successfully synthesized by substituting mechanical stirring during hydrothermal process with ultrasonic irradiation. Difference in physicochemical and optical properties of the $CoAl_2O_4$ pigments prepared by an ultrasonic-assisted-hydrothermal method was characterized using simultaneous thermo-gravimetric and differential thermal analysis (TG–DTA), X-ray diffraction (XRD), field emission scanning electron microscopy (FESEM), high-resolution transmission electron microscopy (HRTEM), diffuse reflectance spectroscopy, CIELAB colorimetric analysis, and testing in ceramic glazes and bodies. The ultrasonic-assisted $CoAl_2O_4$ pigments present a narrow particle size distribution with vivid blue color, and better thermal stability, allowing their use for ceramic inks processed at high temperature. Application of ultrasonic irradiation during the hydrothermal process produces nano-sized powders with better physicochemical and optical properties.

Keywords: Nano-sized pigment; $CoAl_2O_4$; Hydrothermal method; Ultrasonic irradiation; Mechanical stirring

1. Introduction

Inorganic pigments synthesized in nano-size are an integral part of many decorative and protective coatings and used for the coloration of ceramic materials including glazes, clay bodies, and porcelain enamels [1–4]. Nano-sized pigments have a considerable market potential due to their high surface area, which assures higher surface coverage, and high number of reflectance points, hence improved scattering. Recently, demand for tile products with high resolution images has been remarkably increased in the market. From this aspect inkjet printing has advantages as a decoration tool in the porcelain tile field; it is a non-contact method based on projecting ink droplets onto a surface, which permits better control of the image quality and good efficiency of ink usage [5,6]. The use of nano-sized pigments in an ink-jet printing system can overcome problems caused by currently available micron-sized pigments (e.g., nozzle clogging and dispersion instability) and improve the image quality, ensuring high reliability of the printing system [1,5–7]. The nano-sized pigments less than 100 nm perform satisfactorily in preliminary printing tests on ceramic tiles, generating intense colors in a wide range of firing temperatures.

Cobalt aluminate ($CoAl_2O_4$) has received significant attention as a coloring agent in glaze and bulk tile compositions due to its superior properties, such as high refractive index, chemical and thermal stability, and color stability [7–12]. $CoAl_2O_4$ is a transition metal spinel structure that falls into the category of normal spinel with Al in octahedral sites and Co in tetrahedral ones. Solution chemical synthesis techniques are preferably employed for nano-sized $CoAl_2O_4$ powders. The merit of a solution technique is the quasi-atomic dispersion of the component cations in liquid precursors, which facilitates synthesis of a nano-sized crystallite powder with high purity at low temperatures. The hydrothermal process as a solution technique is applicable to synthesize nano-sized and phase-pure

* Corresponding author. Tel.: +82 31 645 1432, fax: +82 31 645 1488.
E-mail address: jino.kim@kicet.re.kr (J.-H. Kim).

0272-8842/$36.00
http://dx.doi.org/10.1016/j.ceramint.2012.04.015

powders from simple and inexpensive precursors without high temperature calcinations in a single experimental step. Therefore, a hydrothermal method has been investigated to synthesize nano-sized $CoAl_2O_4$ in preceding studies [8,9,13].

Despite efficient synthesis of nano-sized pigments by a hydrothermal method, researchers are still frustrated by the severe agglomeration of the resultant inorganic particles. Agglomeration of nano-sized pigments may cause severe problems in ink-jet printing such as nozzle clogging and poor coloring performance. The sonochemical reaction is regarded as originating from acoustic cavitation, the rapid expansion and collapse of bubbles as sound waves pulse through a liquid [14–18]. The cavitation process consists of the creation, growth, and implosive collapse of gas vacuoles in a solution. The ultrasonic treatment as a sonochemical process was used to improve the dispersion of metallic powders and the modification process without deterioration of the final material properties. The resultant particles prepared under ultrasonic treatment generally presented an increase in the specific surface area and the number of defect sites in the solid, leading to a higher basicity [19].

This study aims at synthesizing ceramic blue nano-pigments of $CoAl_2O_4$, using an ultrasonic-assisted hydrothermal method. Ultrasonic irradiation, as a sonochemical process, was applied to prepare well-dispersed $CoAl_2O_4$ nano-pigments in a hydrothermal method, replacing a conventional mechanical stirring. The effect of ultrasonic irradiation on the optical property and thermal stability of synthesized $CoAl_2O_4$ was investigated in detail and compared to those prepared with the mechanical stirring process. The compatibility of nano-sized pigment with transparent glaze was also investigated in the firing process of tiles.

2. Experimental procedure

A 200 ml aqueous nitrate solution of Co-Al ($Co(NO_3)_2{\cdot}6H_2O$, $Al(NO_3)_3{\cdot}9H_2O$, Aldrich Corp.) with a molar ratio of 1:2 was divided into two equal parts. Either under ultrasonic treatment or magnetic stirring at 150 rpm, 3 M NaOH solution was added dropwise to titrate the Co-Al precursor solutions until the pH was reached to 8.5. Then, 50 ml of feedstock was transferred into a Teflon-lined autoclave and treated hydrothermally for 24 h at 250 °C. The probe-type ultrasonicator (UW2070, BANDLIN, the frequency of the ultrasonic wave was 20 kHz) was operated for 30 s at a power of 0.3 kW, followed by an interval of 30 s. After the hydrothermal reaction, the resultant was filtered off, washed with distilled water, and then dried overnight at 80 °C.

The hydrothermally prepared powders were characterized for phase analysis (XRD, D/MAX2500VL/PC, Rigaku, Japan), thermal properties (TG–DTA, DTG-60H, Shimadzu), and microstructure (TEM, Tecnai G2/F30/S-Twin, AP Tech.). In XRD analysis standard silicon was used as a reference to define the FWHM (full width at half maximum) values. Measured peak widths were used in Debye Scherrer's equation to evaluate crystallite sizes. The zeta (ξ) potential of powders in aqueous medium was analyzed by adjusting the pH with nitric acid and sodium hydroxide. The thermal stability and chemical resistance of the hydrothermally prepared powders were investigated by observing the appearance after firing. Glazes with incremental addition of pigments (0.5–3 wt%) were applied on porcelain tile bodies and fired at 1200 °C for 1 h. The composition of the base glaze is summarized in Table 1. Structural and morphological characterizations were conducted by field emission scanning electron microscopy (FESEM, JEOL JSM 6701F) operating at an acceleration voltage of 10 kV and high-resolution transmission electron microscopy (HRTEM, Tecnai G2 F30 S-Twin) operating at 300 kV. In order to assure the optical property of hydrothermally prepared pigments and fired samples with glaze, the CIELAB color measurements were also performed using a spectrophotometer (CARY 100, VARIN). This method used the reflectance data in the visible region to obtain the three relevant parameters, $L^*a^*b^*$, indicating the brightness, red-green, and yellow-blue hue intensities, respectively. Additionally, the diffuse reflectance spectroscopy was conducted with a Perkin-Elmer spectrophotometer in the 200–1000 nm range using a $BaSO_4$ integrating sphere and white reference material.

Table 1
The composition (wt%) of transparent glaze used in this experiment (LOI: loss on ignition).

Composition (wt%)								
SiO_2	Al_2O_3	MgO	CaO	Na_2O	K_2O	Fe_2O_3	TiO_2	LOI
62.5	11.6	0.31	10.4	2.62	2.31	0.22	0.01	9.9

3. Results and discussion

The X-ray diffraction patterns of hydrothermally prepared $CoAl_2O_4$ powders with ultrasonic treatment and mechanical stirring are shown in Fig. 1. Synthesized $CoAl_2O_4$ pigment powders consist of pure spinel phase. The final product of Co–Al composition was strongly influenced by the temperature and the alkaline condition of the hydrothermal treatment [10]. The

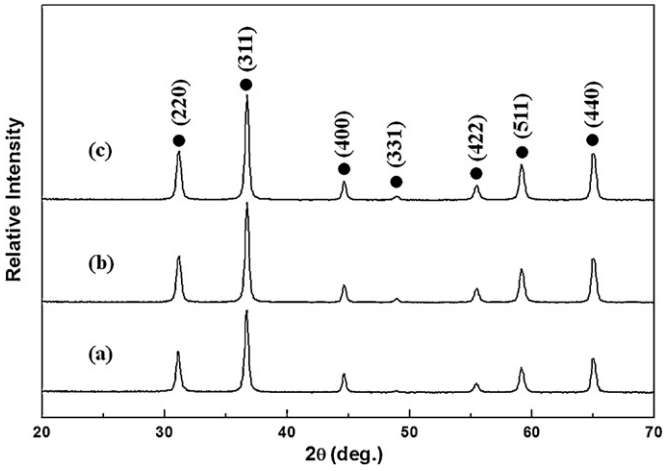

Fig. 1. XRD patterns hydrothermally prepared $CoAl_2O_4$ powders: (a) ultrasonic irradiation, (b) mechanical stirring and (c) ultrasonic irradiation after heat treatment at 1100 °C (●: $CoAl_2O_4$).

Table 2
Structural parameters of hydrothermally prepared $CoAl_2O_4$ powders with ultrasonic irradiation (as-received and annealed) and mechanical stirring.

	$I_{(3\ 1\ 1)}/I_{(2\ 2\ 0)}$	a (Å)	$FWHM_{(3\ 1\ 1)}$
Ultrasonic treatment	2.14	2.13	0.358
Mechanical stirring	2.02	2.11	0.416
Ultrasonic irradiation after heat treatment	2.16	2.15	0.353

$Co_{1-x}Al_x$ layered double hydroxide and the amorphous $Al(OH)_3$ were indicated as impurities at the lower temperature of hydrothermal treatment. In addition, the use of ammonia ($NH_3{\cdot}H_2O$) as a base agent accelerated the formation of $Co_{1-x}Al_x$ layered double hydroxide instead of $CoAl_2O_4$ spinel phase. In our experiment, after the hydrothermal reaction, $CoAl_2O_4$ phase was only detected under the condition of ultrasonic treatment and conventional mechanical stirring. The structure parameters of hydrothermally prepared powders by ultrasonic treatment and mechanical stirring are summarized in Table 2. The intensity ratio of $I_{(3\ 1\ 1)}/I_{(2\ 2\ 0)}$ of the ultrasonic-assisted sample is 2.14 and mechanical stirred sample is 2.02, which can be interpreted as a lower level of cation mixing in the ultrasonic treatment [18,20]. Additionally, the $FWHM_{(3\ 1\ 1)}$ of the ultrasonic-assisted powders is smaller than that of mechanical stirred powders, indicating a better crystallinity in ultrasonic treatment. Therefore, it can be assumed that the introduction of ultrasonic irradiation to the hydrothermal method is beneficial to synthesizing a nano-sized $CoAl_2O_4$ pigment with well-defined crystallinity. It is also important to examine the thermal stability of $CoAl_2O_4$ pigment during glazing process at high temperature. It can be directly judged by looking at the phase stability after heat treatment simulating the high temperature glazing process. For hydrothermally $CoAl_2O_4$ powders with ultrasonic irradiation, any indication of new phase formation was not shown after heat treatment at 1100 °C, although a small increase in peak intensity was observed as shown in Fig. 1(c).

The surface morphology and particle size distribution of the pigment are important factors with respect to the optical property and the dispersion in a medium. HRTEM analysis on the hydrothermally $CoAl_2O_4$ powders with ultrasonic treatment and mechanical stirring are presented in Fig. 2. Fig. 2(a) shows that the ultrasonic-assisted powder has a uniform square morphology with narrow size distribution. Mean particle size is less 100 nm. In contrast, mechanically stirred $CoAl_2O_4$ pigment reveals an irregular structure with wide size distribution from 100 to 200 nm; see Fig. 2(b). The uniform decrease of particle size in the ultrasonic-assisted process can be explained by the deagglomeration of solid powders due to the cavitation effect in the solution with ultrasonic irradiation [18]. The crystallite size of powders prepared by ultrasonic irradiation and mechanical stirring was around 48 nm and 76 nm, respectively, as shown in Fig. 1. Also, the selective area electron diffraction (SAED) pattern of the ultrasonic-assisted powder shows a clear spot pattern without ring patterns, indicating the formation of a well-crystallized $CoAl_2O_4$ phase with a spinel structure, as shown in figure inset in Fig. 2(a). However, the SAED pattern of $CoAl_2O_4$ with mechanical stirring seen from the inset of Fig. 2(b) shows blurred ring as

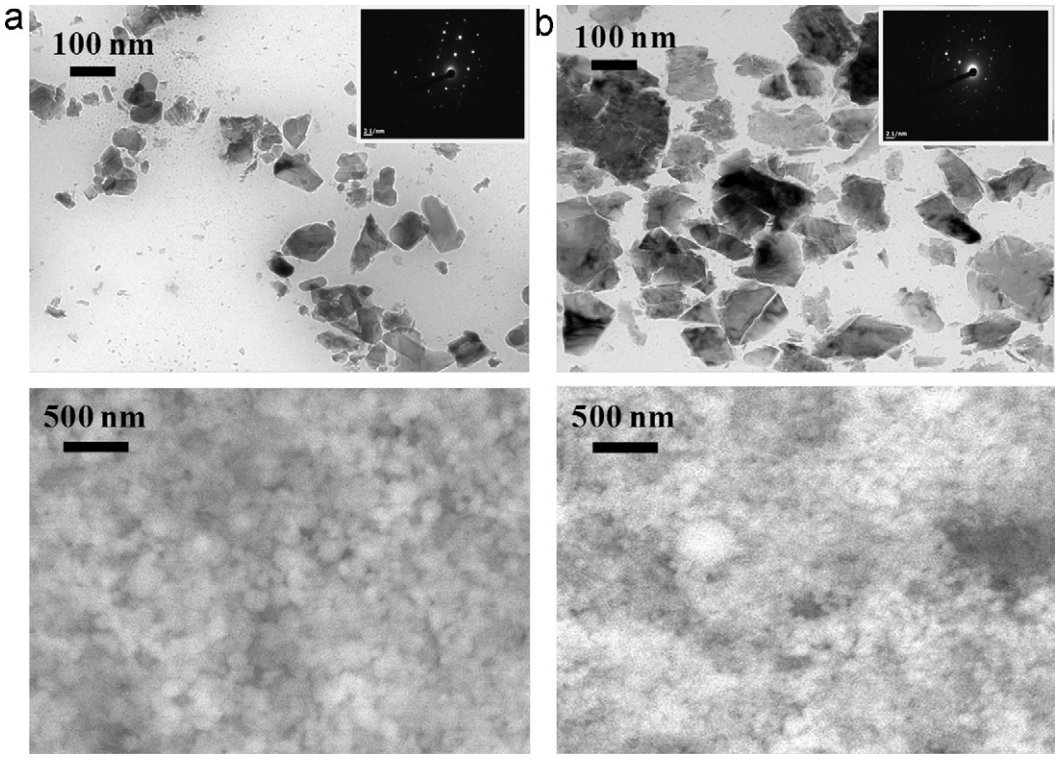

Fig. 2. Microstructural analysis of hydrothermally prepared $CoAl_2O_4$ powders: (a) ultrasonic treatment and (b) mechanical stirring (inset: SAED pattern).

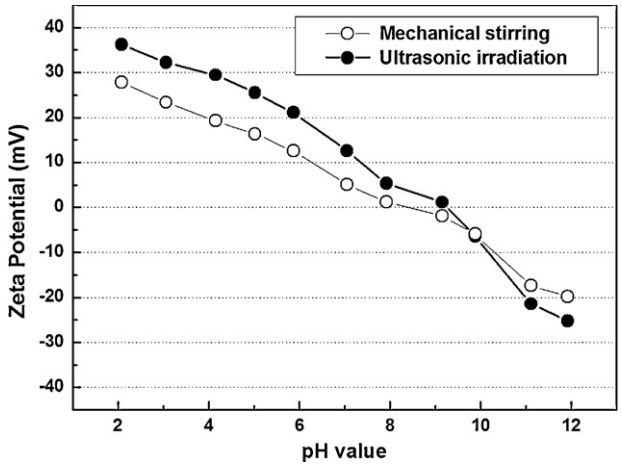

Fig. 3. Change in zeta (ξ) potential with pH value for hydrothermal synthesized $CoAl_2O_4$ nanopowders.

well as spot pattern, which suggests the existence of a polycrystalline composite nature in the synthesized products.

Although the primary particle size of pigments is quite small, their high surface energy causes them to agglomerate during the synthesis and post-synthesis processes. The stability of dispersions is generally determined by measuring the zeta (ξ) potential. Zeta potential can provide a qualitative measure of surface charge on the colloidal particles in a medium. Fig. 3 shows the zeta (ξ) potential variation with pH for hydrothermally $CoAl_2O_4$ with ultrasonic irradiation and mechanical stirring. The isoelectric points (IEP), the pH at which the zeta potential is zero, for $CoAl_2O_4$ nanopowders with ultrasonic irradiation and mechanical stirring were 9.2 and 8.1, respectively. This indicates that particles are more positively charged and have less anionic ions on the surface. Decreasing the strength of H^+ (increasing the pH value) expands the repulsive forces resulting in a sable dispersion of nanopartices [21,22]. The criterion for dispersion stability is established to be $|\xi| > 30$ mV. At more than 30 mV or less than -30 mV, particles strongly repel each other and obtain a stable dispersion. In Fig. 3, the $CoAl_2O_4$ nanopowders with ultrasonic irradiation show much higher absolute zeta potential, $|\xi|$, than those with mechanical stirring. Zeta potential of ultrasonic assisted powders exceed 30 mV at $pH < 3$ while the mechanically stirred $CoAl_2O_4$ nanopowders did not reach the zeta potential stability limit through the measured pH range. Thus, to form a stable dispersion in aqueous medium, the ultrasonic treatment for synthesizing $CoAl_2O_4$ nanopowders would be more effective in comparison to the conventional mechanical stirring.

We investigated the thermal behavior of nano-sized $CoAl_2O_4$ powders using TG–DTA measurement, as shown in Fig. 4. The sample prepared by conventional mechanical stirring shows two endothermic peaks at 530 °C and 1060 °C, respectively, in Fig. 4(a). Two weight loss stages were appeared on the TGA curve with a total weight loss of 7%. Chen et al. reported that the $CoAl_2O_4$ powders prepared by a hydrothermal method has two endothermic reactions, the dehydration of γ-AlO(OH) to γ-Al_2O_3 and the phase transformation of γ-Al_2O_3 to θ-Al_2O_3, respectively [8]. Therefore, it can be assumed that a small amount of γ-AlO(OH) presents in the mechanically stirred product below the detection limit of XRD analysis. On the other hand, there exist no peaks in the DTA curve with a small weight loss of 3 wt% in the TGA curve for ultrasonic-assisted $CoAl_2O_4$ powders, as shown in Fig. 4(b). This suggests single phase formation of $CoAl_2O_4$ and thermal stability without any phase transformation up to 1200 °C. In addition to having a more uniform dispersion of nano-sized particles, the ultrasonic treatment contributed to the homogenization of precursors, leading to the formation of a pure final product.

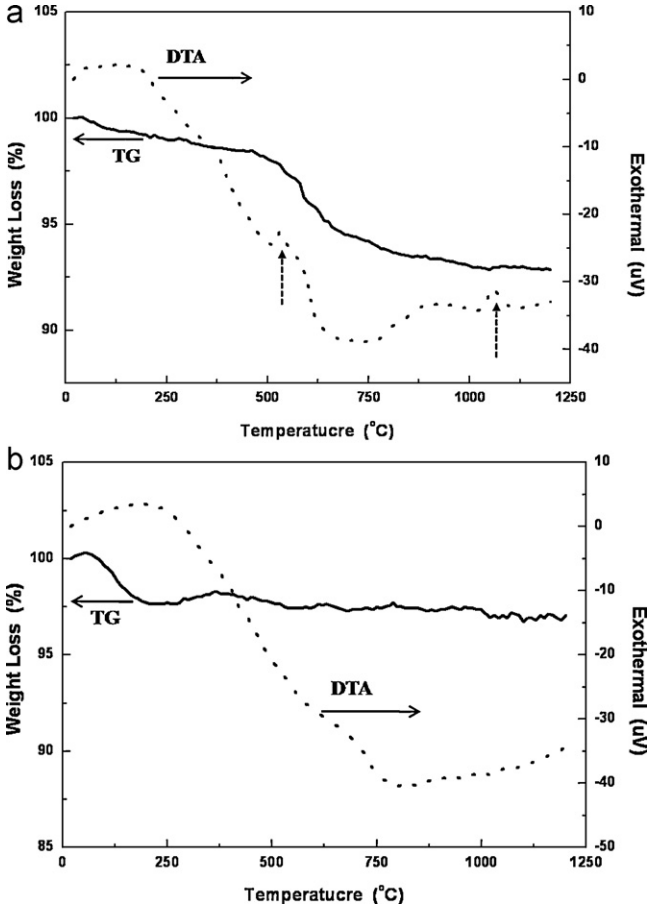

Fig. 4. DTA–TG curves of $CoAl_2O_4$ powders: (a) mechanical stirring and (b) ultrasonic irradiation.

$CoAl_2O_4$ pigment is widely used in the ceramic industry as a blue coloring agent in glazes and the bulk coloration of porcelain stoneware tiles. The UV–visible spectra of ultrasonic-assisted and mechanical stirred powders are shown in Fig. 5. For both samples, the minimum absorption was around 500 nm and the maximum absorption was around 550–660 nm. These values are in good agreement with previously published data [1,8]. Nano-sized $CoAl_2O_4$ is expected to have a spinel-type structure, with Co^{2+} situated at the tetrahedral site. According to the literature, the transition for Co^{2+} ions in a tetrahedral site shows that the two first spin-allowed bands fall in the infrared region (ca. 1400 and 1600 nm), and only the third one is present in the visible region, usually as a triple band around 540 nm (green region), 590 nm (yellow-orange region), and 640 nm

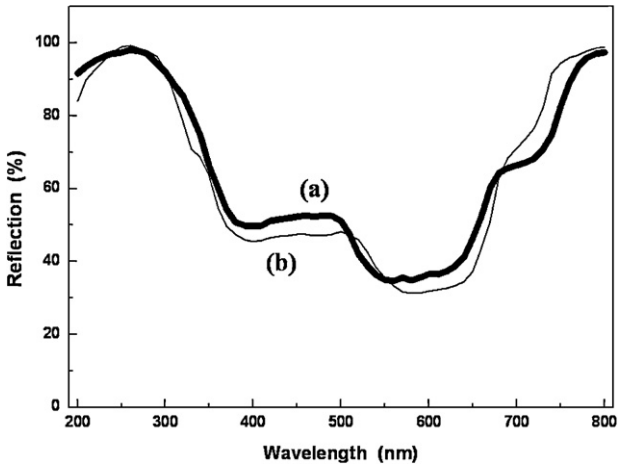

Fig. 5. UV–vis spectrum of $CoAl_2O_4$ powders: (a) mechanical stirring and (b) ultrasonic irradiation.

(red region), which gives rise to the blue color [23]. Under careful identification of UV–visible spectra in Fig. 5, both samples had the same maximum absorption, but the minimum absorption of the ultrasonic-assisted powder was found toward longer wavelengths, indicating that the absorption behavior might be affected by the crystallite and the particle size [8].

The colorimetry analysis, i.e. L^*, a^*, b^* values, on glazes prepared with incremental amount of pigment is summarized in Table 3. The yield of blue color is mainly governed by the parameter b^*: the more b^* value increases in negative the more intense blue color generates. On the other hand, the coordinate L^* gives us the lightness of the pigment (the higher L^*, the lighter), also being an indirect measurement of brightness or intensity of the pigment (the lower L^*, the brighter or more intense the color). In our experiment, more intense blue color was achieved in the ultrasonic-assisted $CoAl_2O_4$ samples as indicated by the extremely high blue component ($b^* = -26.1$) and a relatively low green component ($a^* = -5.8$). The color changes in glaze with the variation of the pigment amount were well evidenced by the evolution of colorimetric parameters. It was noticeable that the difference between the values obtained from the samples with various $CoAl_2O_4$ pigment concentration was more significant compared to those between the ultrasonic-assisted and mechanical stirred pigments. Fig. 6 shows the colors developed by glazes containing ultrasonic-assisted $CoAl_2O_4$ pigment of 0.5 and 3 wt% and the blue color strongly depends on the pigment amount in a glaze.

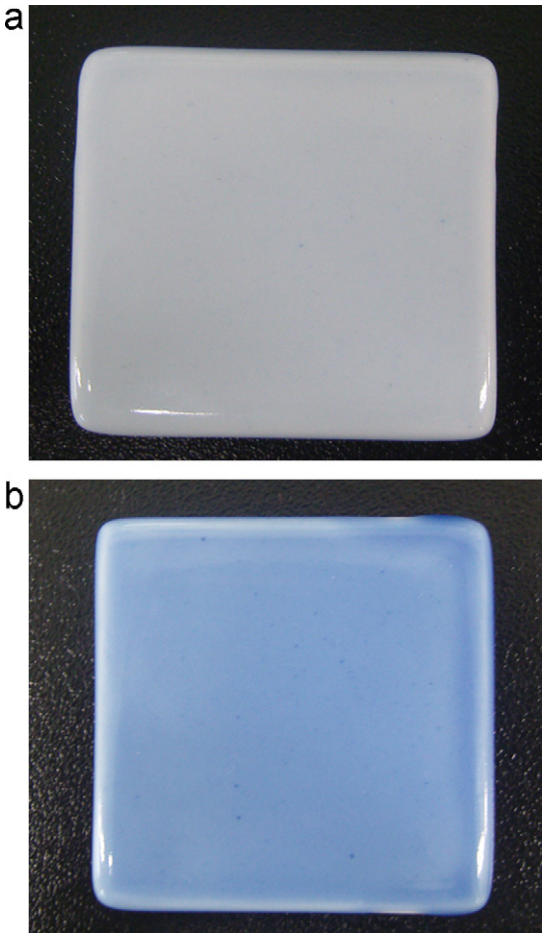

Fig. 6. Ultrasonic-assisted $CoAl_2O_4$ nano-pigment in glaze after heat treatment at 1200 °C for 1 h: (a) 0.5 wt% and (b) 3 wt%.

4. Conclusions

The main results of this study are summarized as follows:

1. Blue ceramic nano-pigment, $CoAl_2O_4$, is successfully synthesized by a hydrothermal method with ultrasonic treatment and mechanical stirring. The introduction of ultrasonic irradiation to the hydrothermal method is beneficial to synthesizing a nano-sized $CoAl_2O_4$ pigment with better crystallinity.
2. The ultrasonic-assisted powder has a uniform square morphology and narrow size distribution with an average particle size of less 100 nm. In contrast, the microscopic morphology of mechanically stirred $CoAl_2O_4$ pigment

Table 3
The colorimetric data for $CoAl_2O_4$ nano-pigments by ultrasonic hydrothermal method; as-synthesized and embedded in the glaze after fast firing at 1200 °C.

	Mechanical stirring					Ultrasonic irradiation				
wt% in glaze	Pigment	0.5	1.0	2.0	3.0	Pigment	0.5	1.0	2.0	3.0
L^*	46.1	73.6	73.4	70.5	72.8	42.3	76.2	72.5	72.6	70.6
a^*	−4.2	−1.1	−1.8	−2.5	−3.7	−5.8	−1.3	−2.6	−3.4	−4.1
b^*	−21.7	−2.0	−6.7	−11.6	−15.6	−26.1	−2.8	−7.3	−12.2	−15.4

implies an irregular structure, with wide size distribution of 100–200 nm. The decrease and uniformity in particle size can be explained by the de-agglomeration of solid powders due to the cavitation effect in the solution with ultrasonic irradiation.

3. There exist no peaks in the DTA curve and small weight loss in the TGA curve for ultrasonic-assisted $CoAl_2O_4$ powders. This suggests pure $CoAl_2O_4$ phase without any phase transformation with temperature. The ultrasonic irradiation during synthesis of nano-sized $CoAl_2O_4$ contributed to the complete blending of precursors, leading to the formation of a pure final product.
4. Both samples had the same maximum absorption, but the minimum absorption of the ultrasonic-assisted powder was found toward longer wavelength. The absorption behavior might be affected by the crystallite size and the particle size.
5. The better blue color was achieved in the ultrasonic-assisted $CoAl_2O_4$ samples as shown by the extremely high blue component ($b^* = -26.1$), a relatively low green component ($a^* = -5.8$) and lower L^* of 42.3.

Acknowledgment

This work was supported from the R&D program by Korea Institute of Ceramic Engineering and Technology.

References

[1] P.M.T. Cavalcante, M. Dondi, G. Guaini, M. Raimondo, G. Baldi, Colour performance of ceramic nano-pigments, Ceramics International 80 (2009) 226–232.
[2] Z. Hu, M. Xue, Q. Zhang, Y. Liu, Nanocolorants: a novel class of colorants the preparation and performance characterization, Dyes and Pigments 76 (2008) 173–178.
[3] N. Sermone, D. Dondi, A. Albini, Inorganic and organic UV filters: their role and efficacy in sunscreens and suncare products, Inorganica Chimica Acta 360 (2007) 794–802.
[4] A.L. Costa, G. Cruciani, M. Dondi, F. Matteucci, New outlooks on ceramic pigments, Industrial Ceramics 23 (2003) 1–11.
[5] D. Gardini, M. Dondi, A.L. Costa, F. Matteucci, M. Blosi, C. Galassi, Nano-sized ceramics inks for drop-on-demand ink-jet printing in quadrichromy, Journal of Nanoscience and Nanotechnology 8 (2008) 1978–1988.
[6] I. Fasaki, K. Siamos, M. Arin, P. Lommens, I. VanDriessche, S.C. Hopkins, B.A. Glowacki, I. Arabazis, Ultrasound assisted preparation of stable water-based nanocrystalline TiO_2 suspensions for photocatalytic applications of inkjet-printed films, Applied Catalysis A – General 411–412 (2012) 60–69.
[7] S. Akdemir, E. Ozel, E. Suvaci, Solubility of blue $CoAl_2O_4$ ceramic pigments in water and diethylene glycol media, Ceramics International 37 (2011) 863–870.
[8] Z. Chen, E. Shi, W. Li, Y. Zheng, W. Zhong, Hydrothermal synthesis and optical property of nano-sized $CoAl_2O_4$ pigment, Materials Letters 55 (2002) 281–284.
[9] Z.Z. Chen, E.W. Shi, W.J. Li, Y.Q. Zheng, J.Y. Zhuang, B. Xiao, L.A. Tang, Preparation of nanosized cobalt aluminate powders by a hydrothermal method, Materials Science and Engineering B 107 (2004) 217–223.
[10] W.S. Cho, M. Kakihana, Crystallization of ceramic pigment $CoAl_2O_4$ nanocrystals from Co–Al metal organic precursor, Journal of Alloys and Compounds 287 (1999) 87–90.
[11] J. Chandradass, M. Balasubramanian, K.H. Kim, Size effect on the magnetic property of $CoAl_2O_4$ nanopowders prepared by reverse miscelle processing, Journal of Alloys and Compounds 506 (2010) 395–399.
[12] C. Wang, S. Liu, L. Liu, X. Bai, Synthesis of cobalt–aluminate spinels via glycine chelated precursors, Materials Chemistry and Physics 96 (2006) 361–370.
[13] F. Yu, J. Yang, J. Ma, J. Du, Y. Zhou, Preparation of nanosized $CoAl_2O_4$ powders by sol–gel and sol–gel hydrothermal methods, Journal of Alloys and Compounds 468 (2009) 443–446.
[14] A. Hassanjani-Roshan, M.R. Vaezi, A. Shokuhfar, Z. Rajabali, Synthesis of iron oxide nanoparticles via sonochemical method and their characterization, Particuology 9 (2011) 95–99.
[15] W. Lu, Q. Qiu, F. Wang, S. Wei, B. Liu, Z. Luo, Sonochemical synthesis of cobalt aluminate nanoparticles under various preparation parameters, Ultrasonics Sonochemistry 17 (2010) 793–801.
[16] M.A. Alavi, A. Morsali, Synthesis of $BaCO_3$ nanostructures by ultrasonic method, Ultrasonics Sonochemistry 15 (2008) 833–838.
[17] S.Y. Yao, Z.H. Xie, Deagglomeration treatment in the synthesis of doped-ceria nanoparticles via coprecipitation route, Journal of Materials Processing Technology 186 (2007) 54–59.
[18] B. Zhang, G. Chen, P. Xu, Z. Lu, Effect of ultrasonic irradiation on the structure and electrochemical properties of cathode material $LiNi_{0.5}Mn_{0.5}O_2$ for lithium batteries, Solid State Ionics 178 (2007) 1230–1234.
[19] A. Perez, F.F. Lamonier, J.M. Giraudon, R. Molina, S. Moreno, Catalytic activity of Co–Mg mixed oxides in the VOC oxidation: effect of ultrasonic assisted in the synthesis, Catalysis Today 176 (2011) 286–291.
[20] W. Li, J.N. Reimers, E. Rossen, J.R. Dahn, In situ X-ray diffraction and electrochemical studies of $Li_{1-x}NiO_2$, Solid State Ionics 67 (1993) 123–130.
[21] N. Mandzy, E. Grulke, T. Druffel, Breakage of TiO_2 agglomerates in electrostatically stabilized aqueous dispersions, Powder Technology 160 (2005) 121–126.
[22] J. Guo, C. Tiu, P.H.T. Uhlherr, T.N. Fang, Yielding behaviour of organically treated anatase TiO_2 suspension, Korea-Australia Rheology Journal 15 (2003) 9–17.
[23] M. Llusar, A. Fores, J.A. Badenes, J. Calbo, M.A. Tena, G. Monros, Colour analysis of some cobalt-based blue pigments, Journal of the European Ceramic Society 21 (2001) 1121–1130.